Sample Preparation-Free, Real-Time Detection of microRNA in Human Serum Using Piezoelectric Cantilever Biosensors at Attomole Level

ARTICLE *in* ANALYTICAL CHEMISTRY · OCTOBER 2012

Impact Factor: 5.64 · DOI: 10.1021/ac303055c · Source: PubMed

2 AUTHORS:

Blake N. Johnson
Virginia Polytechnic Institute and State Univer…
21 PUBLICATIONS **194** CITATIONS
SEE PROFILE

Raj Mutharasan
Drexel University
169 PUBLICATIONS **3,296** CITATIONS
SEE PROFILE

analytical chemistry

Article

pubs.acs.org/ac

Sample Preparation-Free, Real-Time Detection of microRNA in Human Serum Using Piezoelectric Cantilever Biosensors at Attomole Level

Blake N. Johnson and Raj Mutharasan*

Department of Chemical and Biological Engineering, Drexel University, Philadelphia, Pennsylvania 19104, United States

Supporting Information

ABSTRACT: A sensitive, selective, sample preparation-free method for near real-time detection of microRNA in buffer and human serum is given using gold (Au)-coated dynamic piezoelectric cantilever sensors. Sensor response to thiolated DNA probe chemisorption, *hsa-let-7a* hybridization, labeled-DNA hybridization, and Au nanoparticle-functionalized DNA hybridization was monitored continuously in flowing liquid samples using custom flow-cells. The assay showed successful detection of target *let-7a* with a dynamic range spanning 6 orders of magnitude (10 fM−1 nM) with a limit of detection of less than 10 attomoles (~4 fM). The serum background had negligible effect on sensitivity relative to the results obtained in the buffer due to reduction in nonspecific binding caused by continuous sensor vibration. Both hybridization and nonspecific binding reduction were confirmed using fluorescence-based assays to support sensor-based results. The sensor-based method demonstrated excellent selectivity for the microRNA target in comparison with similar microRNA differing by only a single nucleotide (*hsa-let-7c*) and random microRNA sequences. Au nanoparticle-based amplification of sensor response was investigated and led to an order of magnitude improvement in the detection limit and a 128% amplification of sensor response over the entire dynamic range. Au nanoparticle amplification was verified by scanning electron microscopy. The cantilever sensor-based microRNA assay provides competitive sensitivity with current microRNA detection methods and has the advantage of requiring no sample preparation, even when working with biological samples that contain a complex background.

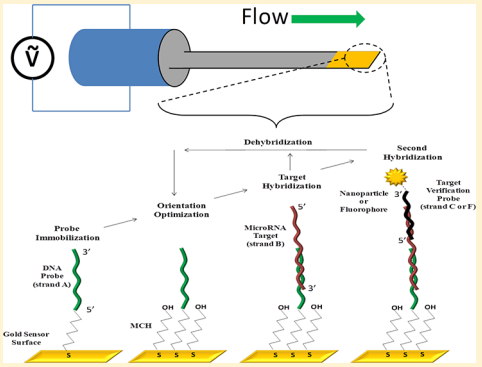

Sensitive measurement of short DNA and RNA strands in liquid is of importance in understanding regulation of gene expression and development of practical medical diagnostics.[1] It is critical that methods for doing so are robust, and selective and minimize sample preparation which contributes to loss or degradation of target species and thus variability of results.[2,3] Particularly, the regulatory role of noncoding microRNAs (~22 base pairs) makes them among such important targets, as their deregulation is associated with various disease states, including cancer. Thus, they provide new opportunities as potential biomarkers if effective techniques for measuring their presence in biological samples can be developed.[4−6] A vast number of microRNAs have been identified in bodily fluids, including urine and blood, which makes sampling for potential diagnostic applications straightforward. Therefore, measuring their presence in liquid samples is a rich diagnostic opportunity.[4−6] Of particular interest is the microRNA *hsa-let-7a* due to association of its aberrant expression with various human diseases, including chronic lymphocytic leukemia (CLL), lung cancer, and breast cancer.[7,8]

Various techniques for measuring microRNA have been investigated. They differ in the time required for analysis, detection limit, dynamic range, selectivity, and required sample preparation. Given microRNA expression has shown to be both up-regulated and down-regulated in disease states, techniques useful in a point-of-care setting require both a low detection limit and a wide dynamic range.[9] Also, due to a high throughput requirement, techniques that lend themselves to multiplexing and minimal sample preparation are especially important. Given the ease of amplifying a low copy number of long nucleic acid strands by PCR and rolling-circle amplification (RCA), various PCR- and RCA-based strategies have been investigated for amplifying microRNAs.[10,11] Since microRNAs are significantly smaller than typical gene-coding mRNA transcripts, adaptive strategies have been required.[11] It has also been reported that variability among inter-PCR results can arise due to differences in amplification efficiency caused by small differences in primer-target melting temperatures due to variable G-C content among different microRNAs.[12] Such methods also typically require extensive sample preparation to minimize enzyme inhibition. Northern Blot has been highly investigated, but it is limited by its relatively low sensitivity (nM levels), requirement of high amounts of starting total RNA, and use of radioactive reagents.[13] Various other strategies based on microarray,[14] enzyme-linked immunosorbent assay (ELISA),[15] nanoparticles,[16] and spectroscopy[17] have also been investigated, but

Received: October 19, 2012
Accepted: October 28, 2012
Published: October 28, 2012

Table 1. Summary of DNA and RNA Strands Used in This Study

strand	name	sequence	MW (kDa)	modification
A	DNA probe	5′-TTTTTTAACTATACAAC-3′	5.4	5′ thiol−C_6
B	*let-7a*	5′-UGAGGUAGUAGGUUGUAUAGUU-3′	7.1	none
C	verification target	5′-ACTACCTCATTTTTTTTTTTT-3′	6.9	3′ 6-FAM™
D	random target	5′-NNNNNNNNNNNNNNNNNNNNN-3′	7.0	none
E	*let-7c*	5′-UGAGGUAGUAGGUUGUAUGGUU-3′	7.1	none
F	Au NP probe	5′-ACTACCTCATTTTTTTTTT-3′	5.6	3′ thiol−C_3

to a lesser extent. Such method-based approaches have shown impressive detection limits at ∼1−100 fM levels,[16,18−20] but various limitations still exist.[21] For example, it has been reported that poor correlation exists between results obtained using microarray and quantitative reverse transcriptase (qRT)-PCR, which is believed to be due to variation in the relative dynamic ranges and probe design.[21] Such methods are also typically sample-preparation intensive, can have lengthy assay times, and often require modification of the target.[22]

Alternatively, of late, sensor-based approaches have shown significant potential for measuring short DNA and RNA strands at competitively sensitive levels. They also provide label-free protocols, high selectivity, and involve minimal sample preparation. Recently, it was shown that nanopore,[23] silicon nanowire,[24] and electrochemical biosensors[25] could measure microRNA in liquid samples with a sensitivity between ∼10−100 fM. A surface plasmon resonance (SPR)-based approach also showed sensitivity near 10 fM; however, it required an additional assay step of nanoparticle amplification.[26] A different SPR-based approach showed excellent sensitivity of ∼1 picomolar (pM); however, it required secondary binding of DNA−RNA duplex-recognizing antibodies to enhance the sensor response.[27]

It was recently demonstrated that piezoelectric-excited cantilever sensors are capable of measuring DNA hybridization *in situ* with continuously flowing liquid samples.[30] In this work, we present a label- and sample preparation-free method for near real-time detection of *hsa-let-7a* in both buffer and human serum background using piezoelectric cantilever sensors over six concentration decades with a detection limit of less than 10 attomoles (∼ 4 fM). We also show the ability to discriminate between related microRNAs which differ by only a single nucleotide. Various control experiments to confirm detection fidelity were developed which included hybridization, dehybridization, and rehybridization in a continuous fashion, and the use of labeled-complementary DNA hybridization (similar to sandwich binding in ELISA applications). Gold (Au) nanoparticles (NPs) provided visual verification as well as to enhance detection limit, amplify sensor response, and increase dynamic range.

MATERIALS AND METHODS

Piezoelectric Cantilever Sensors. Piezoelectric-excited millimeter cantilever sensors (PEMC) were fabricated using techniques described elsewhere.[28] For in-liquid measurements, sensors were electrically insulated by chemical vapor deposition of 10 μm parylene-c on top of a 20 μm underlying spin-coated polyurethane layer used to promote adhesion. For immobilizing the DNA probe through gold (Au)-thiolate binding chemistry, a 100 nm Au layer was sputtered onto the distal tip of the cantilever (1 mm^2).

Sensing Principle. PEMC sensors give rise to sensitive resonant frequencies that decrease in frequency as cantilever mass increases due to the molecular binding between functionalized surface probes and biochemical targets. The sensor is excited by a sinusoidal electric field along the lead zirconate titanate (PZT) polarization axis (cantilever thickness dimension). Periodic application of an electric field results in periodic cantilever deformation at a frequency equal to the excitation frequency. Mechanical resonant frequencies are identified by maxima locations of the phase angle between the excitation potential and the resulting electric current in PZT caused by higher than normal strains that occur at resonance.[29] The sensor was installed in a custom flow-cell and the resonant frequency was continuously monitored in liquid. By measuring resonant frequency response as molecular binding occurs at various concentrations, it is possible to quantify microRNA levels present in liquid samples. A schematic of the experimental apparatus can be found in Figure S.1 of the Supporting Information.

Data Processing and Statistical Analysis. Raw sensor data was processed by taking the median value of raw data collected every two minutes to reduce measurement noise without compromising rate information. P-values (p) are based on comparison of mean concentration-dependent sensor responses over multiple repeated experiments (n = 3−10 different sensors) with mean sensor response of control experiments involving injections of pure buffer, pure serum, and random microRNA-containing samples. A two-tailed t test was used in all cases.

Reagents. Probe and target sequences are shown in Table 1 along with corresponding end-group modifications and molecular weight. The thiolated DNA probe complementary to the 3′ end of *hsa-let-7a* (strand A), *hsa-let-7a-1* microRNA (strand B), fluorescently labeled verification target (strand C), 22 base pair (bp) random microRNA target (strand D), *hsa-let-7c* microRNA (strand E), and a thiolated Au nanoparticle (NP) DNA probe (strand F) were purchased from Integrated DNA Technologies (IDT, Coralville, IA). Ethylenediaminetetraacetic acid (EDTA) and tris-hydrochloride (Tris-HCl) were from Sigma-Aldrich. Sodium chloride (NaCl), potassium hydroxide (KOH), and sodium hydroxide (NaOH) were from Fisher Scientific. DNA and RNA were reconstituted in Tris-EDTA buffer (10 mM Tris, 1 mM EDTA, pH = 7.9, 1 M NaCl) using sterile diethylpyrocarbonate (DEPC)-treated nuclease-free deionized water (DIW, Fisher Scientific) and stored at −22 °C until being removed immediately before use. Ethanol (EtOH, 200 proof) was from Decon Laboratories, Inc. (King of Prussia, PA). The thiol molecule, 1-mercapto-6-hexanol (MCH), used for Au < 111> site backfilling was from Fluka. Pooled human serum was from Innovative Research, Inc. Concentrated sulfuric acid (H_2SO_4) and hydrogen peroxide (30% v/v, H_2O_2) used for making piranha solution (3:1 v/v H_2SO_4:H_2O_2) were from Fisher Scientific. (Caution: Piranha solution is highly reactive; handle with care.) Bond-Breaker TCEP [tris(2-carboxyethyl)phosphine] solution (500 mM)

dx.doi.org/10.1021/ac303055c | Anal. Chem. 2012, 84, 10426−10436

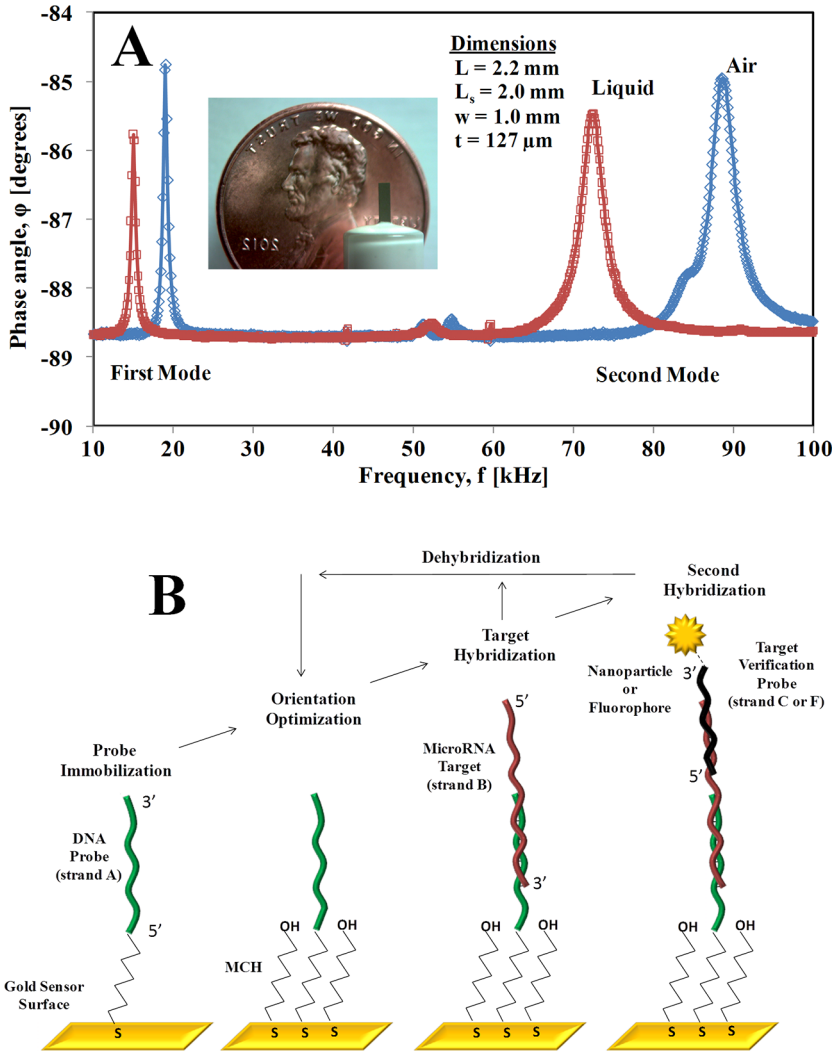

Figure 1. (A) Sensor spectra measured in air and water shows first (n = 1) and second (n = 2) resonant frequencies. The second resonant frequency was used in all molecular sensing experiments. (B) Schematic of cantilever-based assay protocol for detection of microRNA, depicting the main steps of probe immobilization, probe orientation optimization, target hybridization, and target hybridization verification and amplification.

used for reduction of the disulfide form of the DNA probe was from Fisher Scientific. NanoOrange reagent was from Invitrogen-Life Technologies (Grand Island, NY). Gold nanoparticles (15 nm, 2.3 nM Au particle) were from BBInternational (Cardiff, U.K.).

Au Surface Preparation. To ensure efficient thiol immobilization the flow-cell and reagent reservoirs were treated with dilute piranha solution (~1:5 v/v piranha:DIW) prior to all binding experiments and copious EtOH- and DIW-rinse (18 MΩ, Milli-Q system, Millipore). The freshly deposited Au surface was cleaned by immersion in fresh piranha solution for two minutes followed by immersion in a potassium hydroxide–hydrogen peroxide solution (1:1 v/v 0.1 M KOH:30% H_2O_2) for 30 s. The sensor was then rinsed immediately with copious amounts of DIW.

DNA Probe Preparation. Thiolated DNA probe was supplied by the vendor in disulfide form. The disulfide bond was reduced by adding 1 µL of TCEP to 300 µL of a 3 µM probe, mixing, and allowing the mixture to react 60 min at room temperature. The reduced probe was added to the recirculating buffer (flow rate = 800 µL/min) to chemisorb the DNA probe on the Au surface. Flow was maintained using a peristaltic pump. Given that the flow-loop was 2.1 mL and the flow-cell volume was 300 µL, it required ~3 min for the newly introduced reagent to replace the loop volume. Unoccupied Au ⟨111⟩ sites was backfilled by injecting 1 mL of MCH (730 µM) into the flow-loop. Au NPs were functionalized by incubation of 100 µL of stock Au NP solution in 300 µL of a 3 µM DNA probe (strand F) with 1 µL of TCEP for one hour. After one hour, the NPs were washed by centrifugation (14 000 rpm for 30 min) and resuspended in 1 mL of TE buffer.

DNA-RNA Dehybridization. A 1.5 M NaOH aqueous solution was used to dehybridize DNA–RNA duplexes on the sensor as was done in previous studies.[30,31]

Protein Assays. All protein assays were carried out using vendor-supplied protocols for use of the NanoOrange reagent. Freshly cleaned sensors were immersed in 50% human serum for a period of 1 h without exciting the sensor, to allow for nonspecific adsorption of serum proteins to occur. Sensors were then rinsed with DIW to remove loosely bound species and immersed in 500 µL of DIW to effect desorption for a 10 min period. During this 10 min, sensors were either not excited, excited at 10 mV, and excited at 100 mV to examine the effect of vibration on the level of protein released. The level of protein in the DIW was then characterized.

dx.doi.org/10.1021/ac303055c | Anal. Chem. 2012, 84, 10426–10436

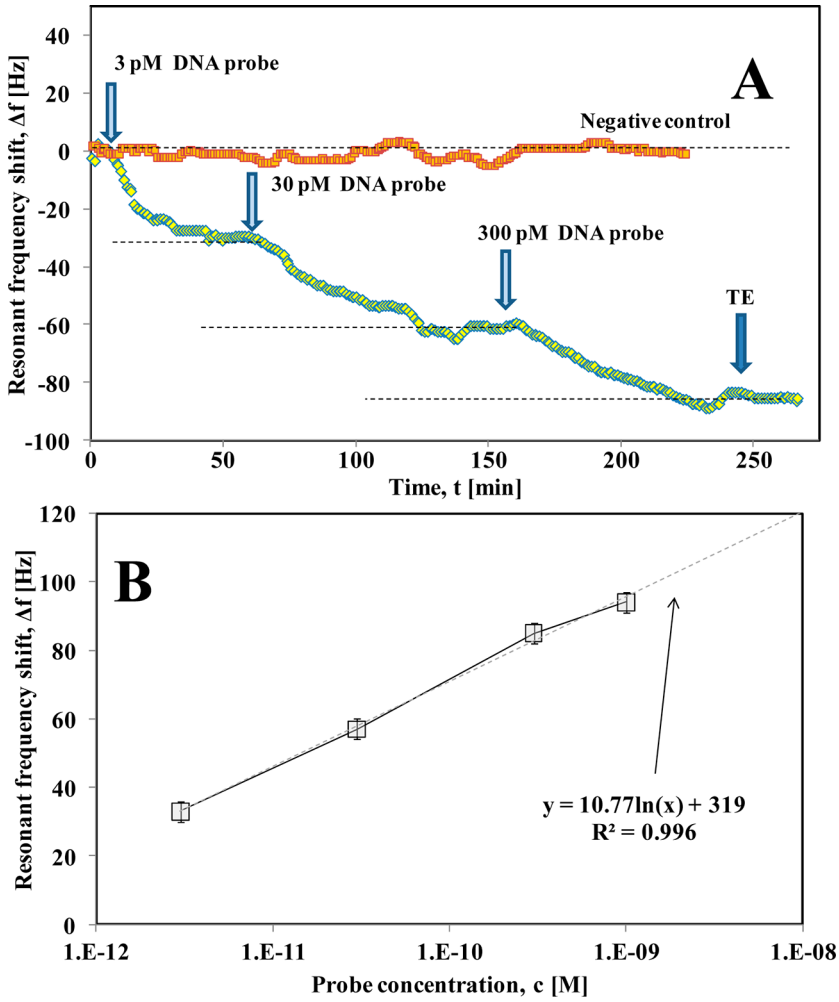

Figure 2. (A) Representative sensor response to sequential concentration-dependent chemisorption responses of the DNA probe (3 pM, 30 pM, and 300 pM). (B) Analysis of sensor response shows excellent reproducibility of the probe immobilization step and the notable log-linear sensitivity relationship. Note, data at 3 nM was gathered from the surface preparation for microRNA hybridization experiments.

RESULTS AND DISCUSSION

Sensor Characteristics and Liquid Immersion Effects. As stated previously in Sensing Principle, the cantilever sensors are excited via application of an alternating 100 mV potential across the PZT thickness (127 μm). Figure 1A shows the measured phase angle as a function of the excitation frequency. The spectrum shows two major resonant frequencies at 19.0 ± 0.1 and 88.4 ± 0.1 kHz, which correspond to the first and second transverse modes of the cantilever, respectively. One significant advantage of millimeter cantilever sensors over smaller micro- and nanoscale dynamic-mode cantilevers is their sustained resonance in liquid. A detailed discussion of their fluid-structure interaction properties has been reported elsewhere.[32] The immersed-sensor frequency response spectrum is also shown in Figure 1A. Immersion in liquid caused a decrease in resonant frequency and Q-value of both modes, primarily through an added-mass effect of the surrounding liquid. The first and second resonant frequencies decreased by 4.2 ± 0.7 and 16.2 ± 1.2 kHz (n = 3 different sensors), respectively, and Q-values decreased by 37 ± 8% (n = 3 different sensors). Such values agreed within 14.4% of theoretically predicted shifts calculated using reported analytical models.[33] We note that various sensors were used in this study which ranged from a total length of L = 2.0−3.0 mm, all of which had similar sensor characteristics. Since cantilever sensor sensitivity increases with resonant frequency,[28] the highest resonant frequency expressed in the 1−100 kHz frequency range was used in microRNA sensing experiments discussed subsequently. We note that the standard deviations are given for both sensor response on single sensors and averaged sensor response from multiple sensors. Demonstrating measurement repeatability using different sensors is paramount in demonstrating fabrication reproducibility and performance properties in sensor-based assays. Standard deviations in the latter case are increased by approximately a factor of 3, due to small variations in resonant frequency among different sensors. Standard deviations and associated p values based on different sensor response discussed in the subsequent text show high reproducibility of sensor characteristics and confidence in the results.

DNA Probe Immobilization. The experimental apparatus consists of reagent vessels joined via a five-port manifold, inlet valves, a custom flow-cell which holds the sensor, and a peristaltic pump, all connected in a flow-loop configuration (see Figure S.1 of the Supporting Information). Such an arrangement enables reagent flow either (1) to go through the loop and into a waste reservoir (once-through format), or (2) to be continuously recirculated (recirculation format). Thus, all assay steps described in Figure 1B were carried out without removing

dx.doi.org/10.1021/ac303055c | Anal. Chem. 2012, 84, 10426−10436

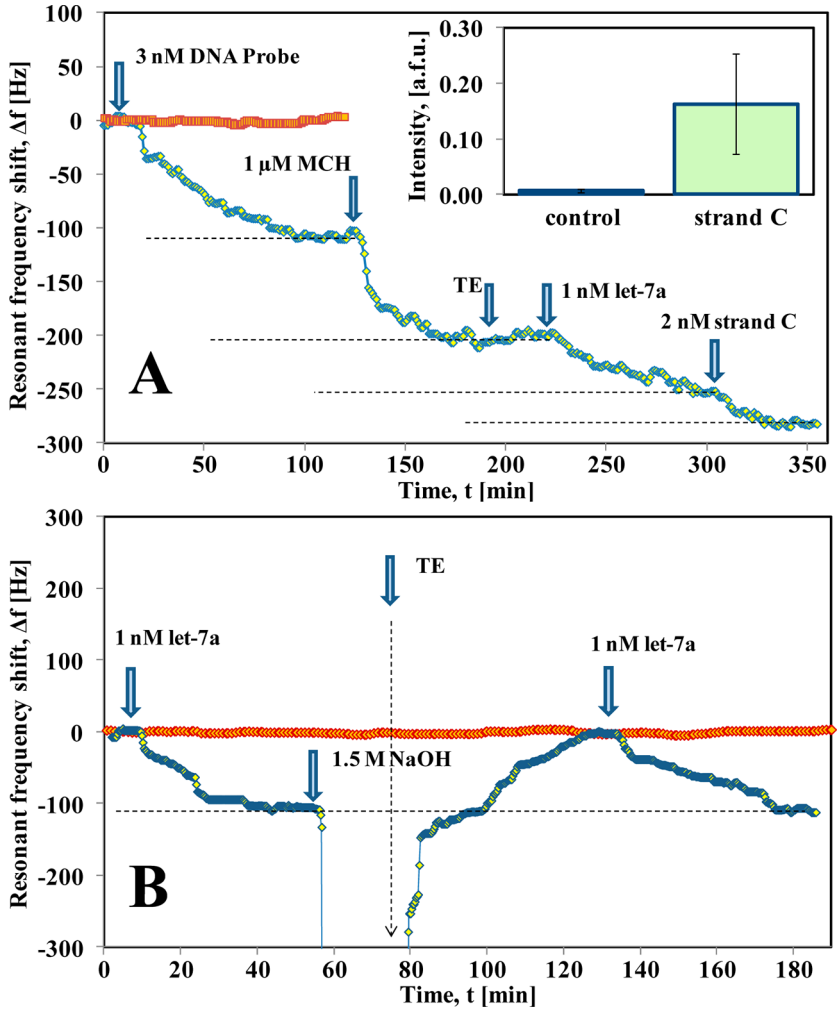

Figure 3. Controls used for verification of microRNA hybridization. (A) Second hybridization of a fluorescently labeled DNA strand (strand C, 100 μL of 2 nM) gives both a small additional added-mass sensor response and a fluorescence signal (see inset). (B) Hybridization (100 μL of 1 nM), dehybridization, and rehybridization of microRNA measured continuously on the sensor.

the sensor from the flowing liquid which eliminates contaminants that may cause false responses.

A typical PEMC sensor coated with 1 mm^2 Au can accommodate a maximum of 4 × 10^{12} DNA probes (6.9 picomoles) based on the average coverage area per thiol molecule (24 Å^2)[34−36] and the assumption of a defect-free Au surface. Given that the molecular weight of the DNA probe used is 5.4 kDa (Table 1), the maximum mass of DNA (m_{sat}) which can be immobilized under ideal circumstances is 36 ng. A detection assay was started by installing the sensor in the flow-cell and establishing a constant flow rate (Q) of the buffer. Once resonant frequency reached steady state, 100 μL of the reduced-DNA probe (3 nM) was injected into the loop, upstream of the sensor. After a slight time delay (i.e., ∼2 min, the time required for the fluid to reach the flow-cell), the sensor resonant frequency decreased due to chemisorption of the DNA probe on the Au < 111> sites.[36] The chemisorption took approximately 60 min to reach equilibrium, which established a new sensor steady state at a lower resonant frequency value. A representative example of sensor response to concentration-dependent probe immobilization is shown in Figure 2A. A decrease in resonant frequency observed was due to added mass on the sensor caused by chemisorption of DNA on Au. Chemisorption of 3 pM DNA (300 attomoles) caused an exponential decrease in the resonant frequency (net shift = −30.2 ± 1.3 Hz) at a rate of 0.073 ± 0.003 min^{-1}. Rates were obtained assuming a first-order rate model during the initial rate period. The observed rate agrees reasonably with previously reported values measured using cantilever sensors.[30,37] After the sensor reached a new steady state post-DNA chemisorption, another injection of the DNA-containing sample was made, but at a higher concentration, and sensor response was monitored. This process was repeated sequentially until the concentration reached 300 pM, after which flow was returned to the TE buffer in a once-through flow format for removing unbound DNA from the flow-loop. In all experiments, the switch to the buffer caused no measurable shift in resonant frequency, indicating that DNA remained bound to the sensor. We also note that the sensor did not respond if the flow-loop was injected with a DNA-free sample, and it also showed no response in the absence of molecular binding (examined over a three hour period, variance = 2.8 Hz). Analysis of the concentration-dependent binding responses (Figure 2A) provided sensitivity data for sensor characterization and is summarized in Figure 2B. Relationship between the probe concentration and net resonant frequency response was log-linear over the four-log concentration range investigated and exhibited a nonlinear behavior near 800 pM due to the

dx.doi.org/10.1021/ac303055c | Anal. Chem. 2012, 84, 10426−10436

onset of surface saturation effects. The log-linear concentration-dependent sensor response has been observed in various sensing platforms.[15,26,30,38] Observed saturation behavior is also a common phenomenon in sensing platforms where the sensing area is finite.[39,40] In all subsequent microRNA hybridization experiments, the DNA probe concentration of 3 nM was used to prepare the Au surface. At this concentration, the DNA probe was introduced near the theoretical saturation limit (~2.1 ng, 300 femtomoles) but still low enough to avoid very high packing of the ssDNA strands which has been shown to inhibit target hybridization,[40] albeit at target concentrations which far exceed those used in low-level detection applications by many orders of magnitude. Previous studies have used similar concentrations for examining low-level detection limits.[30] Exposure to 6-mercapto-1-hexanol (MCH) was carried out post-DNA chemisorption to ensure upright orientation of the immobilized DNA probes (Figure 1B).[37,39] MCH, being a small molecule, occupies the vacant Au < 111> sites, thereby releasing weakly bound negatively charged phosphate backbone and nitrogenous bases of DNA from the sensor surface. We hypothesize that MCH reduces the potential for false positive results that may arise due to nonspecific binding of the background species to a vacant Au surface. Experimental error in this study includes both error associated with the assay itself and variations associated with fabrication of multiple sensors used. All errors presented are that of the former. The interested reader is directed to Figures S.4 and S.5 of the Supporting Information for device-associated variations, which show variability of sensor properties.

Verifying microRNA Hybridization. Prior to examining the dynamic range and detection limit, various control experiments were carried out to verify that sensor response was indeed caused by microRNA hybridization. These verification techniques included (1) measuring the hybridization of a second DNA strand (strand C) that would only occur if the microRNA target had hybridized, somewhat analogous to the sandwich-binding approach used in the ELISA protocols, (2) confirming that a fluorescent signal could be measured on the sensor surface after strand C hybridized, and (3) hybridizing, dehybridizing, and rehybridizing the microRNA target in a continuous fashion.

The principle of second DNA strand (strand C) hybridization to the hanging end of the *let-7a*-DNA probe duplex is shown schematically in Figure 1B. First, injection of 100 μL of a 3 nM DNA probe caused a -113 ± 3 Hz decrease in resonant frequency due to DNA chemisorption. After the new steady state was reached, backfilling of vacant Au sites with MCH caused a further -89 ± 3 Hz shift, but at a more rapid rate than the DNA probe (0.079 ± 0.003 min^{-1}) (Figure 3A). After the sensor response reached a steady state, the flow-loop was flushed with a TE buffer (~15 min) which caused a negligible change in resonant frequency, indicating that the DNA probe and MCH remained bound to the sensor. Subsequently, the flow-loop was injected with 100 μL of *let-7a* sample (100 pM), and flow was placed in recirculation. Hybridization of *let-7a* with a surface-bound DNA probe caused a further 97 ± 3 Hz decrease in resonant frequency. Subsequently, the flow-loop was injected with 100 μL of sample containing the second DNA strand (strand C, 2 nM). Over the course of the next 40 min, the sensor response decreased by an additional 25 ± 3 Hz and ultimately reached a new steady state at a lower resonant frequency value, indicating that the prior binding response was indeed due to *let-7a* hybridization. We note that sensor response was not due to nonspecific binding by comparison with controls discussed in Vibration-Assisted Reduction of Nonspecific Adsorption and Discrimination Against Other let-7 Family Members Differing by a Single Nucleotide. It should be noted that the secondary verification strand could be used as a second reporter strand to examine if single nucleotide differences exist in the overhang region. However, the *let-7* family does not contain sequence variability in the overhang region.[41] The immobilized capture probe was designed to be selective for variation in all but one of the *let-7* family members, and thus strand C is for verification of hybridization and not for reporting of *let-7*a detection.

Given that strand C hybridization confirmed that the earlier response was due to *let-7a* hybridization, fluorescence intensity on the sensor surface was measured after strand C hybridization for further verification. In the inset of Figure 3A, we show a comparison of the fluorescence signals (λ_{ex} = 495 nm, λ_{emis} = 520 nm) measured on both a strand C-hybridized sensor and a control sensor that lacked a hybridized strand C. The two sensors exhibited a significant difference in measured fluorescence intensity (p = 0.03), which provided a further confirmation that the sensor response measured post-*let-7a* injection was indeed due to its hybridization with the surface-bound DNA probe.

As an additional test of fidelity of the sensor response, we examined dehybridization and subsequent rehybridization of *let-7a* on the sensor in a continuous fashion. As previously described, hybridization of *let-7a* (1 nM) was monitored continuously and allowed to reach equilibrium. As shown in Figure 3B, hybridization of the *let-7a* target caused a -103 ± 3 Hz shift in the resonant frequency. Once the sensor response stabilized, the flow was switched to NaOH (1.5 M) in a once-through format to effect dehybridization[30,31] and remove the dehybridized strand from the flow-loop. Switching to NaOH caused a rapid decrease in the resonant frequency due to a higher density of NaOH. After ~20 min, the flow was returned to the TE buffer, and the sensor response was allowed to recover. Switching back to the TE buffer caused a rapid increase in the resonant frequency followed by a slower increase. The initial rapid response was primarily due to density effects, while the subsequent slower response was due to equilibration of temperature gradients caused by initial exothermic heat of mixing between NaOH and the TE buffer. Ultimately, the resonant frequency returned to the initial resonant frequency value, which indicated that the previously hybridized *let-7a* target was completely dehybridized by the alkaline solution. Finally, in order to both confirm the dehybridization and to examine the effects of the alkaline NaOH treatment on the immobilized DNA probe, the flow was returned to a *let-7a*-containing sample at the same concentration as was used initially. As observed previously, the sensor response decreased due to rehybridization of *let-7a* and ultimately reached a new steady state comparable to the first hybridization response within experimental error. We examined repeated NaOH dehybridization and rehybridization up to three cycles and found no degradation in the sensor response or sensor damage suggesting that the sensor can be used repeatedly without required cleaning and removal from the flow cell. In other studies, the NaOH dehybridization technique was shown to be successful over 50 cycles.[31]

Detection Limit in Buffer. The detection limit of *let-7a* in the buffer was measured by hybridization responses of *let-7a*-containing samples in which target concentrations ranged from

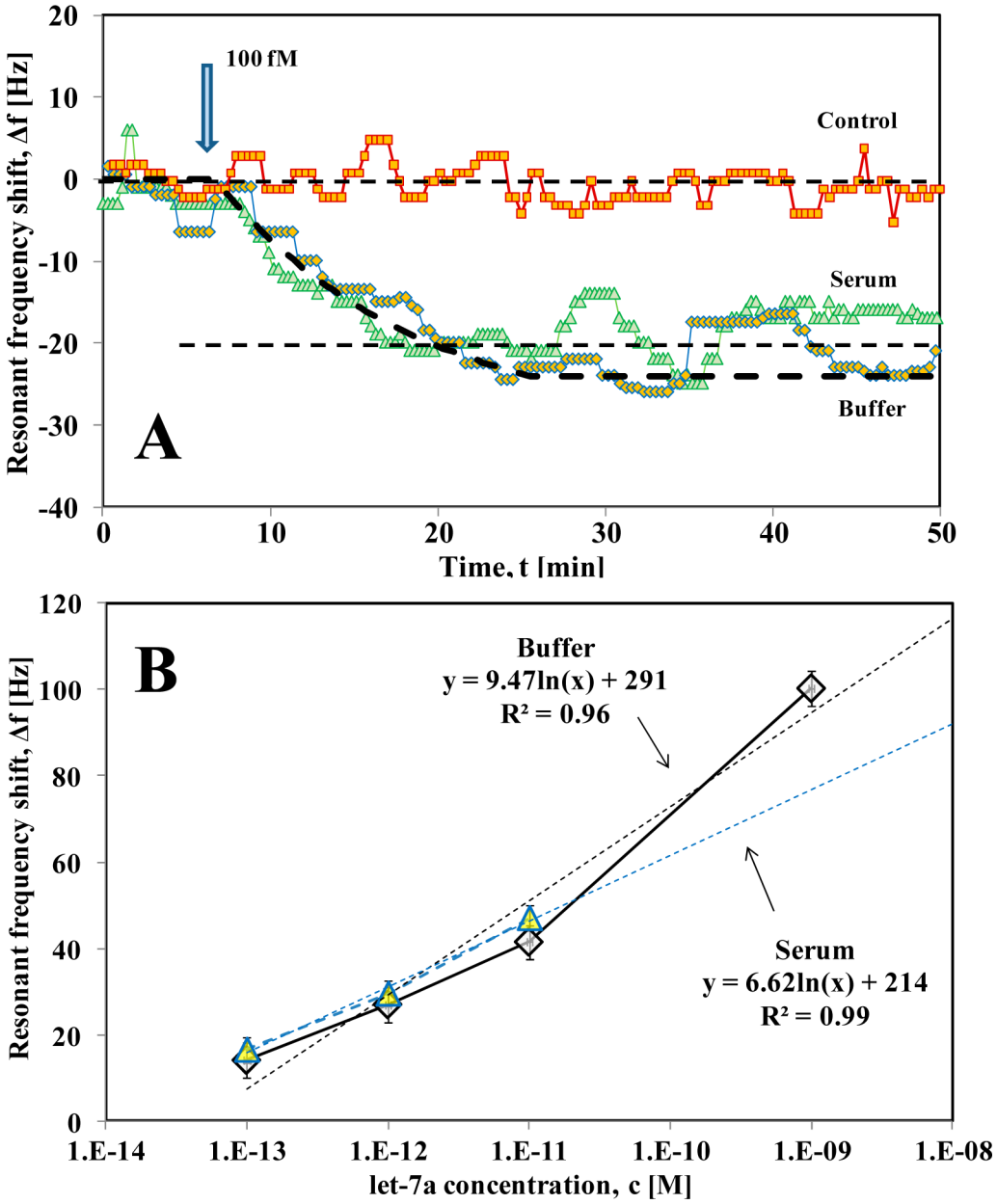

Figure 4. (A) Comparison of hybridization responses measured at 100 fM in both buffer and serum. (B) Summary of sensor response to *let-7a* hybridization in the buffer and serum.

100 fM−1 nM. After DNA probe chemisorption and MCH backfilling steps, injection of 100 μL of 100 fM *let-7a*-containing sample caused the resonant frequency to decrease 15.9 ± 2.9 Hz and ultimately reach a new steady state at the lower resonant frequency value (Figure 4A). After equilibrium was reached, successively higher concentration of the *let-7a* sample was injected into the loop in a similar fashion as was done during concentration-dependent DNA probe chemisorption experiments (DNA Probe Immobilization), and the sensor response was measured. This enabled sensor response to *let-7a* hybridization over the 100 fM−1 nM concentration range to be obtained. Figure 4B shows the net resonant frequency response as a function of *let-7a* concentration. Similar to the trend of sensor response observed for DNA probe immobilization, the response to *let-7a* detection was also log-linear. The lowest concentration examined was 100 fM, which caused a reproducible shift of 14.1 ± 6.7 Hz (n = 5 different sensors, p = 0.03). In 100 μL of a 100 fM *let-7a* sample there are 10 attomoles of microRNA target, which indicates that the assay has reproducible sensitivity at attomole levels. In reality, it is unlikely that all 10 attomoles hybridized, but an equilibrium fraction of bound and unbound strands existed involving less than 10 attomoles in the bound state. This implies that the sensitivity estimate is conservative. Nevertheless, we use the 10 attomole value to estimate absolute mass-change sensitivity. This suggests that the assay is capable of detecting microRNA, which are present even at the lower level under physiological conditions (~15 fM).[42]

Detection Limit in Serum. The sensor response to *let-7a* hybridization was then examined in 50% human serum in TE buffer as it provides a protein-containing background, relevant in a diagnostic setting. Thus, the experiments discussed in Detection Limit in Buffer were repeated in 50% serum instead of the TE buffer. After the DNA probe and MCH were

dx.doi.org/10.1021/ac303055c | *Anal. Chem.* 2012, 84, 10426−10436

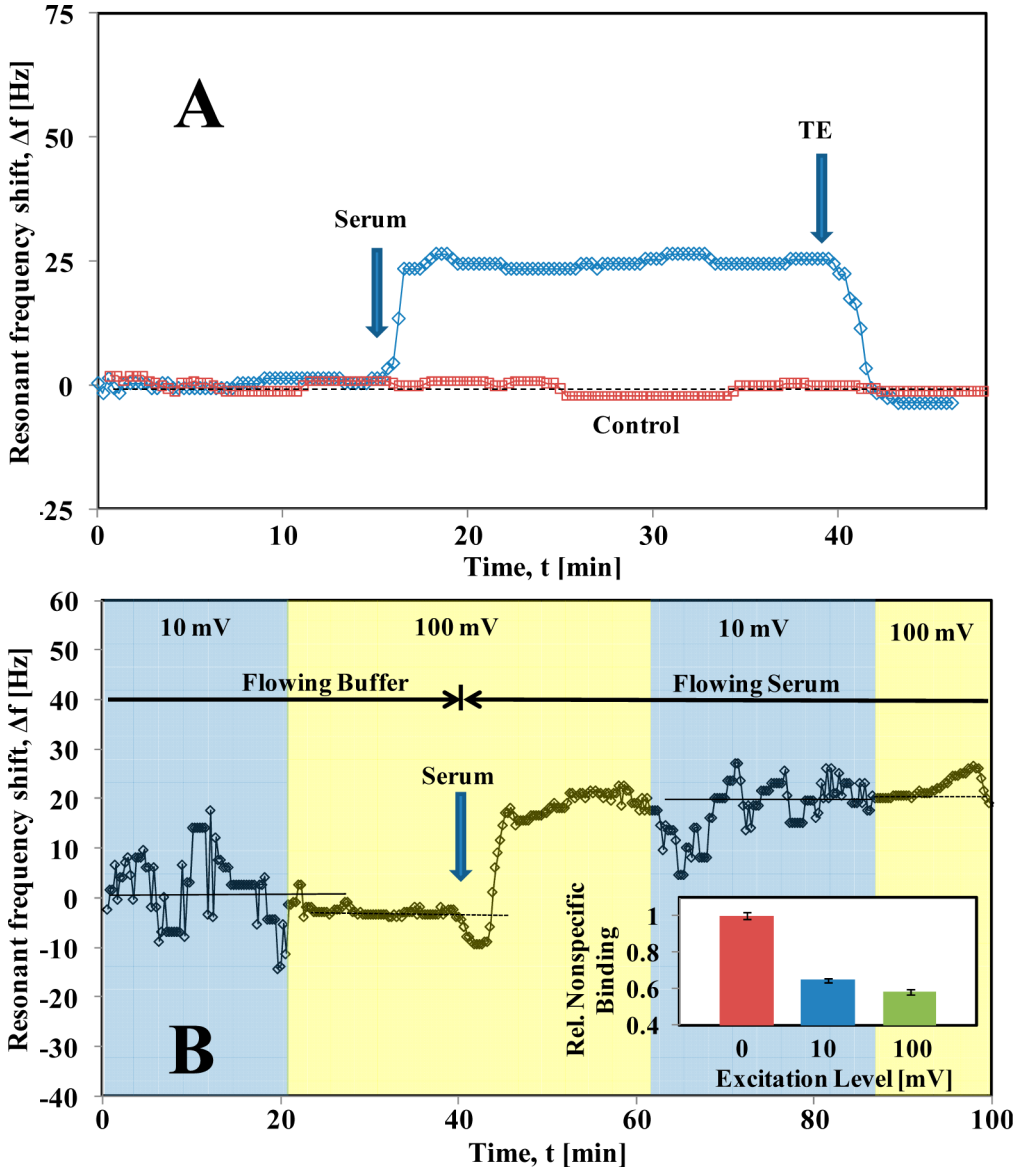

Figure 5. (A) Sensor response to flowing serum at 100 mV of excitation used for all detection experiments shows negligible nonspecific binding effects. (B) Nonspecific binding effects on sensor response at various excitation values shows the ability of the vibration to cause the reduction of the nonspecific binding of serum proteins. See the inset for the level of reduced nonspecific binding in reference to the static sensor based on the fluorescence measurements.

immobilized in the TE buffer, flow was changed to 50% serum in a once-through format to completely replace the TE buffer in the loop. Subsequently, flow was returned to the recirculation format, and resonant frequency was allowed to reach steady state. Similar to the buffer experiments, 100 μL of a 100 fM *let-7a*-containing sample diluted by a factor of 2 using 100% serum was injected in the flow-loop and allowed to hybridize. Likewise, after the sensor response reached steady state post-hybridization, the higher concentration of the *let-7a*-containing sample was sequentially injected and sensor responses were measured. Net sensor responses obtained in 50% serum are compared in Figure 4 with results obtained in the buffer. Interestingly, the responses obtained in 50% serum were within experimental error of experiments conducted in buffer, suggesting that the detection assay is not significantly affected by the serum background. The reason for the minimal effect of serum background on sensitivity is analyzed further in the following section. For comparison of buffer- and serum-based detection results, in Figure 4A we show the sensor responses measured at the lowest concentration examined (100 fM) in both backgrounds. Both cases involved similar transient periods of 25 min and net resonant frequency shifts of 21.7 ± 3.1 and 17.8 ± 3.0 Hz for the buffer and serum, respectively.

Vibration-Assisted Reduction of Nonspecific Adsorption. Existing literature suggests that surface vibration may provide resistance to nonspecific adsorption.[43−45] Since PEMC sensors vibrate continuously at resonance during sensing, it was of interest to examine whether or not vibration may have contributed to the nearly identical hybridization results obtained in both buffer and serum, by minimizing nonspecific adsorption of the background protein. Since the sensor is excited at 100 mV, we were interested in determining if the response to the serum background was modulated by the level of excitation voltage. However, prior to examining voltage-dependence on sensor response in the serum, we first carried out control studies at a fixed excitation voltage (100 mV).

dx.doi.org/10.1021/ac303055c | *Anal. Chem.* 2012, 84, 10426−10436

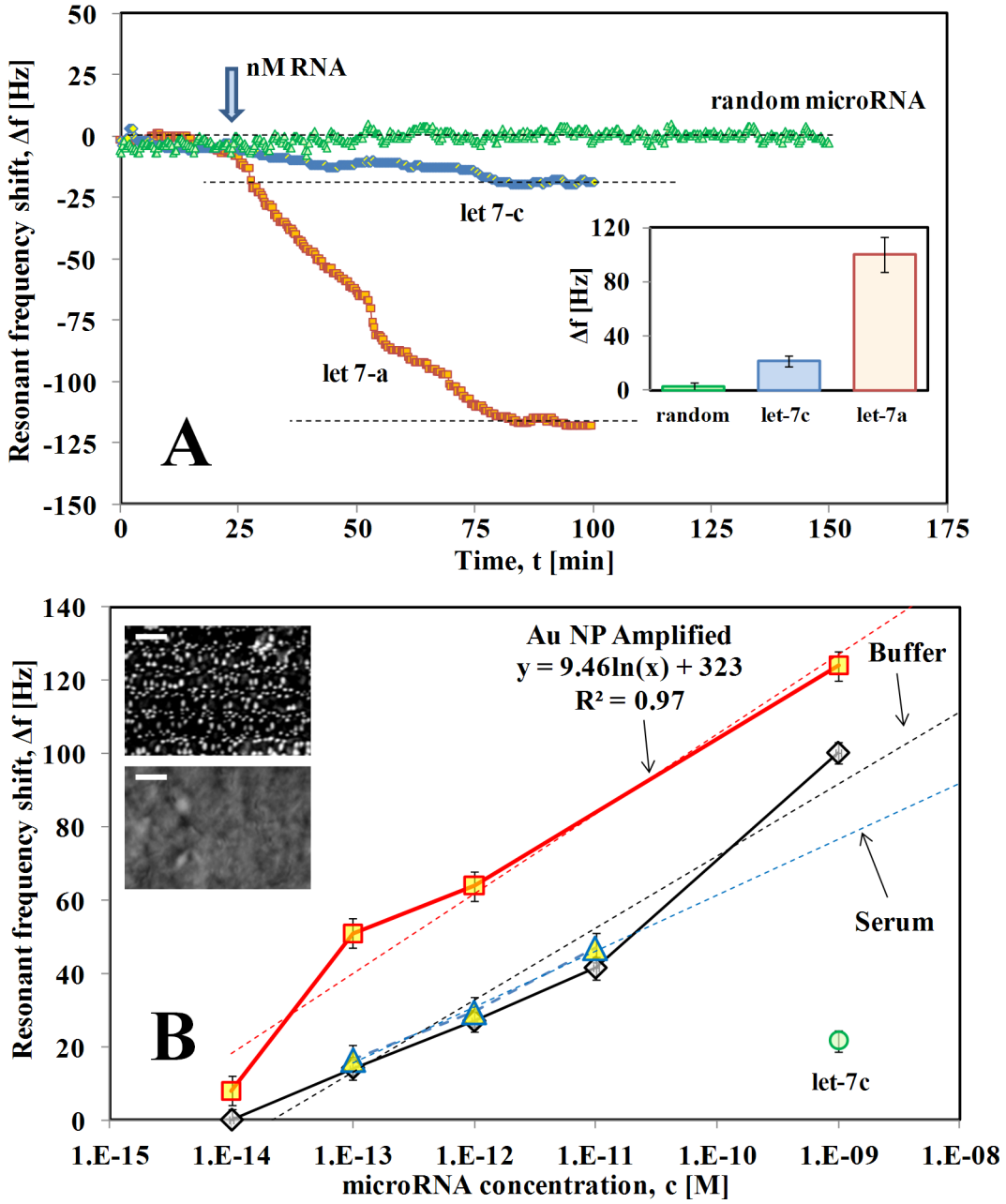

Figure 6. (A) Selectivity for discriminating among related microRNA with single nucleotide polymorphism. (B) Comparison of NP-amplified responses with those obtained NP-free in the buffer. The inset shows an SEM micrograph of the Au surface which was amplified with the Au NP technique (scale bar = 100 nm).

Figure 5A shows the DNA-functionalized sensor response to change in flow between the TE buffer and the 50% serum. Once the serum reached the flow-cell, the resonant frequency increased, due to the density decrease relative to the TE buffer. After a short transient period, the resonant frequency reached a new steady state, 27.4 ± 1.4 Hz (n = 3 different sensors) above its previous value. After 30 min, the flow was returned to the TE buffer, which caused the sensor response to rapidly decrease due to the density change and ultimately reach a new steady state within the experimental error of the initial resonant frequency value. The absence of a net resonant frequency shift greater than the sensor noise relative to the initial steady state suggests that at 100 mV excitation nonspecific binding effects are reduced to such an extent that they cause no significant change in sensor response.

Since intensity of vibration is proportional to the excitation voltage, it was of interest to see if the nonspecific adsorption increased if excitation voltage was reduced. Therefore, the excitation voltage was reduced to 10 mV, and nonspecific adsorption effects were likewise examined by changing between the flow of buffer and serum. Figure 5B shows the sensor response caused by changing between the different excitation voltages when the flow was either buffer or serum. When the flow was the protein-free buffer, the change in excitation voltage from 10 to 100 mV (the voltage used in all detection studies) caused a small decrease in the resonant frequency (4.9 ± 0.7 Hz). However, when the flowing medium was protein-containing serum, change in the excitation voltage from 10 to 100 mV caused no measurable decrease in the resonant frequency. This difference suggests that (1) a small level of

dx.doi.org/10.1021/ac303055c | Anal. Chem. 2012, 84, 10426−10436

nonspecific binding occurred in the serum during the time in which the sensor was excited at the lower excitation voltage, and (2) returning the excitation voltage to the higher value released nonspecifically bound species that adsorbed at a lower excitation voltage. For further verification that higher excitation voltage reduced nonspecific adsorption, we carried out fluorescence-based assays to assess the level of removal of nonspecifically bound proteins at different excitation voltages. In these studies, the unexcited, static sensors were immersed in 50% serum for 1 h to allow nonspecific binding to occur. The sensor was then rinsed and transferred to a pure DIW-containing reservoir for 10 min to effect desorption of nonspecifically adsorbed serum proteins from the sensor, thus establishing a reference for comparison with measurements obtained while the sensor was vibrated. The protein level in the sample was then measured. To examine the effects of vibration and voltage excitation on the level of released protein, the experiment was repeated while exciting the sensor at either 10 or 100 mV during the desorption period. The inset of Figure 5B shows a comparison of reduction in nonspecific binding as a function of the excitation voltage. Even at 10 mV, the vibration led to a reduced nonspecific binding but not to the extent achieved at 100 mV. Thus, the data suggest that the sensor vibration clearly reduces nonspecific binding, thus contributing to the ability to make highly sensitive measurements in the serum.

Discrimination Against Other *let-7* Family Members Differing by a Single Nucleotide. Given the high probability that a practical microRNA sensing assay contains additional microRNA species, some of which may differ from the target by only a single nucleotide known as a single nucleotide polymorphism (SNP), it is important to examine the assay selectivity for such cases. Thus, the sensor response to the SNP-target *let-7c*-containing samples (1 nM) was measured (see Table 1). Figure 6A shows a comparison of the sensor response obtained when a freshly prepared DNA-functionalized sensor was exposed to *let-7a*, *let-7c*, or random microRNA strands. Although the DNA probe was fully complementary only to the *let-7a* target, a small hybridization response was observed with the *let-7c*-containing sample (21.7 ± 4.2 Hz; $p < 0.01$; $n = 3$ different sensors). However, the response was significantly lower than the hybridization response of the *let-7a* target (100.2 ± 13.4 Hz, $p < 0.01$, $n = 5$ different sensors). Such a result is consistent with other microRNA sensing assays.[17,19] The random target-containing samples (5 nM) caused no measurable shift in the resonant frequency. Thus, the use of a multiple sensor assay, in which additional sensors are functionalized with complementary probes against potential microRNAs which differ by a single base pair, could easily distinguish between the SNP response and that due to low concentration of target microRNA.

Amplification of Sensor Response Using Gold Nanoparticles. NPs can be used to amplify sensor response on mass-based sensing platforms.[46] Thus, experiments were conducted to examine if binding of Au NPs to already hybridized *let-7a* strands could be used as such a technique. We first began with a low concentration sample at the log-linear-predicted detection limit. After immobilizing the DNA probe and backfilling with MCH, the sensor was exposed to 10 fM *let-7a* in the same fashion as was described previously. No significant sensor response was observed over a 45 min period indicating that the added-mass (~7 fg) was too small to induce a sensor response. After the 45 min, one mL of strand F-functionalized Au NPs was injected into the loop which caused an 8.0 ± 3.6 Hz ($n = 3$ different sensors) decrease in resonant frequency over the next 80 min due to Au NP binding to the existing DNA probe-*let-7a* duplexes which had formed over the previous 45 min. Assuming a 1:1 binding stoichiometry between Au NPs and the hybridized *let-7a* strands ($N \sim 6 \times 10^5$), the maximum possible NP-added mass was 20.4 pg. This amplification method was then repeated at a higher concentration of *let-7a*. Au NP binding responses and expanded verifying scanning electron micrographs can be found in Figures S.2 and S.3, respectively, of the Supporting Information. The cumulative data, summarized in Figure 6B, shows that the Au NP amplification caused a 128% increase in sensor response over the concentration range tested, which is similar to the amplification observed in other studies.[47,48] Au NPs increased the dynamic range by an order of magnitude. A slight increase in noise associated with the measurement is thought to be due to additional assay steps involved in Au NP preparation discussed in Materials and Methods. We remind the reader that the use of Au NP is only required to measure microRNA concentrations of 10 fM. The data suggest that, while assay sensitivity is high without amplifying NPs, the added hybridization with a second complementary strand labeled with Au NPs improved both sensitivity and fidelity of the assay. On the basis of a minimally resolvable signal-to-noise ratio of three and the measured noise level of 2.8 Hz, the concentration-based limit of detection in the buffer is estimated to be 4 fM.

■ CONCLUSION

Piezoelectric cantilever sensors provided sensitive, selective, and sample preparation-free detection of the *let-7a* microRNA in both buffer and human serum at competitive levels, with existing techniques for microRNA detection. A significant advantage is the assay is free of sample preparation. Dynamic range spanned 6 orders of magnitude, and the limit of detection was less than 10 attomoles (~4 fM). The serum background was found to have a negligible effect on sensitivity, which was shown to be due to the ability of sensor vibration to significantly reduce nonspecific adsorption effects. The assay also carries sufficient selectively to differentiate between alternative microRNA species differing by only a single nucleotide. Gold nanoparticle-labeled complementary strand amplified sensor response, dynamic range, and limit of detection.

■ ASSOCIATED CONTENT

Supporting Information

A schematic of the experimental apparatus (Figure S.1), sensor response to gold nanoparticle (Au NP) amplification of *let-7a* (Figure S.2), and scanning electron micrographs of Au NP-amplified samples versus Au control samples are given (Figure S.3). We also present the reproducibility of the laboratory-fabricated cantilever sensors design, whereby we include the fabrication-associated error instead of the assay-associated error which is presented in the main body of the manuscript (Figures S.4 and S.5). This material is available free of charge via the Internet at http://pubs.acs.org.

■ AUTHOR INFORMATION

Corresponding Author

*E-mail: mutharasan@drexel.edu. Tel: (215) 895-2236. Fax: (215) 895-5837.

Notes

The authors declare no competing financial interest.

■ ACKNOWLEDGMENTS

The authors are grateful for the generous support of the NSF Grant CBET-0828987 which provided the entire funding for this work.

■ REFERENCES

(1) Cissell, K. A.; Deo, S. K. *Anal. Bioanal. Chem.* **2009**, *394* (4), 1109−1116.
(2) Keilholz, U.; Willhauck, M.; Rimoldi, D.; Brasseur, F.; Dummer, W.; Rass, K.; de Vries, T.; Blaheta, J.; Voit, C.; Lethé, B.; Burchill, S. *Eur. J. Cancer* **1998**, *34* (5), 750−753.
(3) Ladanyi, A.; Molnar, B.; Soong, R.; Tabiti, K.; Tulassay, Z. *Clin. Chem. (Washington, DC, U.S.)* **2001**, *47* (10), 1860−1862.
(4) Chen, X.; Zhang, J. F.; Zen, K.; Zhang, C. Y. *MicroRNAs as Blood-Based Biomarkers of Cancer*; Springer: New York, 2011; p 499−532.
(5) Reid, G.; Kirschner, M. B.; van Zandwijk, N. *Crit. Rev. Oncol. Hematol.* **2011**, *80* (2), 193−208.
(6) Yu, D. C.; Li, Q. G.; Ding, X. W.; Ding, Y. T. *Int. J. Mol. Sci.* **2011**, *12* (3), 2055−2063.
(7) Bartels, C. L.; Tsongalis, G. J. *Clin. Chem. (Washington, DC, U.S.)* **2009**, *55* (4), 623−631.
(8) Heneghan, H. M.; Miller, N.; Lowery, A. J.; Sweeney, K. J.; Newell, J.; Kerin, M. J. *Ann. Surg.* **2010**, *251* (3), 499−505.
(9) Calin, G. A.; Croce, C. M. *Nat. Rev. Cancer* **2006**, *6* (11), 857−866.
(10) Schmittgen, T. D.; Lee, E. J.; Jiang, J.; Sarkar, A.; Yang, L.; Elton, T. S.; Chen, C. *Methods* **2008**, *44* (1), 31−38.
(11) Benes, V.; Castoldi, M. *Methods* **2010**, *50* (4), 244−249.
(12) Jing, H.; Song, Q.; Chen, Z.; Zou, B.; Chen, C.; Zhu, M.; Zhou, G.; Kajiyama, T.; Kambara, H. *Chem. BioChem.* **2011**, *12* (6), 845−849.
(13) Li, W.; Ruan, K. *Anal. Bioanal. Chem.* **2009**, *394* (4), 1117−1124.
(14) Bissels, U.; Wild, S.; Tomiuk, S.; Holste, A.; Hafner, M.; Tuschl, T.; Bosio, A. *RNA* **2009**, *15* (12), 2375−2384.
(15) Cissell, K. A.; Rahimi, Y.; Shrestha, S.; Hunt, E. A.; Deo, S. K. *Anal. Chem.* **2008**, *80* (7), 2319−2325.
(16) Yang, W.-J.; Li, X.-B.; Li, Y.-Y.; Zhao, L.-F.; He, W.-L.; Gao, Y.-Q.; Wan, Y.-J.; Xia, W.; Chen, T.; Zheng, H.; Li, M.; Xu, S.-q. *Anal. Biochem.* **2008**, *376* (2), 183−188.
(17) Bi, S.; Zhang, J.; Hao, S.; Ding, C.; Zhang, S. *Anal. Chem.* **2011**, *83* (10), 3696−3702.
(18) Raymond, C. K.; Roberts, B. S.; Garrette-Engele, P.; Lim, L. P.; Johnson, J. M. *RNA* **2005**, *11* (11), 1737−1744.
(19) Cheng, Y.; Zhang, X.; Li, Z.; Jiao, X.; Wang, Y.; Zhang, Y. *Angew. Chem.* **2009**, *121* (18), 3318−3322.
(20) Li, J.; Schachermeyer, S.; Wang, Y.; Yin, Y.; Zhong, W. *Anal. Chem.* **2009**, *81* (23), 9723−9729.
(21) Koshiol, J.; Wang, E.; Zhao, Y. D.; Marincola, F.; Landi, M. T. *Cancer Epidemiol. Biomark. Preven.* **2010**, *19* (4), 907−911.
(22) Wegman, D. W.; Krylov, S. N. *Angew. Chem.* **2011**, *123* (44), 10519−10523.
(23) Wang, Y.; Zheng, D.; Tan, Q.; Wang, M. X.; Gu, L.-Q. *Nat. Nanotechnol.* **2011**, *6* (10), 668−674.
(24) Zhang, G.-J.; Chua, J. H.; Chee, R.-E.; Agarwal, A.; Wong, S. M. *Biosens. Bioelectron.* **2009**, *24* (8), 2504−2508.
(25) Gao, Z.; Yang, Z. *Anal. Chem.* **2006**, *78* (5), 1470−1477.
(26) Fang, S.; Lee, H. J.; Wark, A. W.; Corn, R. M. *J. Am. Chem. Soc.* **2006**, *128* (43), 14044−14046.
(27) Šípová, H.; Zhang, S.; Dudley, A. e. M.; Galas, D.; Wang, K.; Homola, J. i. *Anal. Chem.* **2010**, *82* (24), 10110−10115.
(28) Sharma, H.; Lakshmanan, R. S.; Johnson, B. N.; Mutharasan, R. *Sens. Actuators B* **2011**, *153* (1), 64−70.
(29) Johnson, B. N.; Mutharasan, R. *Sens. Actuators, B* **2011**, *155* (2), 868−877.
(30) Rijal, K.; Mutharasan, R. *Anal. Chem.* **2007**, *79* (19), 7392−7400.
(31) Lazerges, M.; Perrot, H.; Rabehagasoa, N.; Compère, C.; Dreanno, C.; Mucio Pedroso, M.; Faria, R. C.; Bueno, P. R. *Sens. Actuators, B* **2012**, *171−172* (0), 522−527.
(32) Johnson, B. N.; Mutharasan, R. *J. Appl. Phys.* **2011**, *109* (6), 066105.
(33) Van Eysden, C. A.; Sader, J. E. *J. Appl. Phys.* **2006**, *100* (11), 114916.
(34) Schreiber, F. *Prog. Surf. Sci.* **2000**, *65* (5−8), 151−257.
(35) McKendry, R.; Zhang, J. Y.; Arntz, Y.; Strunz, T.; Hegner, M.; Lang, H. P.; Baller, M. K.; Certa, U.; Meyer, E.; Guntherodt, H. J.; Gerber, C. *Proc. Natl. Acad. Sci. U.S.A.* **2002**, *99* (15), 9783−9788.
(36) Love, J. C.; Estroff, L. A.; Kriebel, J. K.; Nuzzo, R. G.; Whitesides, G. M. *Chem. Rev. (Washington, DC, U.S.)* **2005**, *105* (4), 1103−1170.
(37) Calleja, M.; Nordström, M.; Álvarez, M.; Tamayo, J.; Lechuga, L. M.; Boisen, A. *Ultramicroscopy* **2005**, *105* (1−4), 215−222.
(38) Li, J.; Yao, B.; Huang, H.; Wang, Z.; Sun, C.; Fan, Y.; Chang, Q.; Li, S.; Wang, X.; Xi, J. *Anal. Chem.* **2009**, *81* (13), 5446−5451.
(39) Kjällman, T. H. M.; Peng, H.; Soeller, C.; Travas-Sejdic, J. *Anal. Chem.* **2008**, *80* (24), 9460−9466.
(40) Peterson, A. W.; Heaton, R. J.; Georgiadis, R. M. *Nucleic Acids Res.* **2001**, *29* (24), 5163−5168.
(41) Griffiths-Jones, S.; Grocock, R. J.; van Dongen, S.; Bateman, A.; Enright, A. J. *Nucleic Acids Res.* **2006**, *34*, D140−D144.
(42) Mitchell, P. S.; Parkin, R. K.; Kroh, E. M.; Fritz, B. R.; Wyman, S. K.; Pogosova-Agadjanyan, E. L.; Peterson, A.; Noteboom, J.; O'Briant, K. C.; Allen, A.; Lin, D. W.; Urban, N.; Drescher, C. W.; Knudsen, B. S.; Stirewalt, D. L.; Gentleman, R.; Vessella, R. L.; Nelson, P. S.; Martin, D. B.; Tewari, M. *Proc. Natl. Acad. Sci. U.S.A.* **2008**, *105* (30), 10513−10518.
(43) Yeh, P.-Y. J.; Kizhakkedathu, J. N.; Madden, J. D.; Chiao, M. *Colloids Surf., B* **2007**, *59* (1), 67−73.
(44) Yeh, P.; Le, Y.; Kizhakkedathu, J.; Chiao, M. *Biomed. Microdevices* **2008**, *10* (5), 701−708.
(45) Cular, S.; Branch, D. W.; Bhethanabotla, V. R.; Meyer, G. D.; Craighead, H. G. *Sensors Journal* **2008**, *8* (3), 314−320.
(46) Liu, T.; Tang, J. a.; Jiang, L. *Biochem. Biophys. Res. Commun.* **2004**, *313* (1), 3−7.
(47) Mao, X.; Yang, L.; Su, X.-L.; Li, Y. *Biosens. Bioelectron.* **2006**, *21* (7), 1178−1185.
(48) Hao, R.-Z.; Song, H.-B.; Zuo, G.-M.; Yang, R.-F.; Wei, H.-P.; Wang, D.-B.; Cui, Z.-Q.; Zhang, Z.; Cheng, Z.-X.; Zhang, X.-E. *Biosens. Bioelectron.* **2011**, *26* (8), 3398−3404.